Proceedings of the ASME 2025
Structures, Structural Dynamics, and Materials Conference
SSDM2025
May 5-7, 2025, Houston, TX, USA

SSDM2025-152001

DYNAMIC STIFFNESS METHOD FOR FREE VIBRATION OF BEAMS AND FRAMEWORKS USING HIGHER ORDER SHEAR DEFORMATION THEORY

J Ranjan Banerjee

Department of Engineering, School of Science and Technology
City St George's, University of London, Northampton Square, London EC1V 0HB, UK

ABSTRACT

The dynamic stiffness method for free vibration of beams and frameworks is developed using a higher order shear deformation theory. Starting with the displacement field, the potential and kinetic energies of the beam in flexural vibration, are first formulated. Then, Hamilton's principle is applied to derive the governing differential equations and associated natural boundary conditions. Next, the differential equations are solved to obtain the expressions for flexural displacement, bending rotation and the first derivative of the flexural displacement. The expressions for the shear force, bending moment and the higher-order moment are obtained from the natural boundary conditions resulting from the Hamiltonian formulation. Finally, the force vector comprising the amplitudes of the shear force, bending moment and the higher-order moment is related to the amplitudes of the displacement vector comprising the flexural displacement, bending rotation and the first derivative of the flexural displacement through the frequency-dependent dynamic stiffness matrix. The dynamic stiffness matrix for axial motion which is uncoupled from the flexural motion is now implemented to the dynamic stiffness matrix in flexural motion to analyse individual beams and frameworks for their free vibration characteristics by applying the Wittrick-Willaims algorithm. Illustrative examples are given, and significant conclusions are drawn.

Keywords: dynamic stiffness method, higher order shear deformation theory, beams, frames, Wittrick-Williams algorithm

1. INTRODUCTION

The earliest beam theory that we know of, was developed in the eighteenth century by Euler and Bernoulli [1, 2]. The theory endured the test of time remarkably well, and is still being used satisfactorily, even to this day. The theory, known as the Bernoulli-Euler or Euler-Bernoulli beam theory, was further improved about a century later by Lord Rayleigh [3] who included the effect of the rotatory inertia of the beam cross-section which improved the accuracy of results, and this was demonstrated by Searle [4]. This relatively unknown Rayleigh-beam theory was overshadowed by the theory developed by Timoshenko and Ehrenfest in the earlier part of the twentieth century [5, 6] when they considered both the effects of rotatory inertia and shear deformation and advanced the Bernoulli-Euler beam theory significantly. The rest is essentially an impactful history which is a continuing account of the applications and developments of the Timoshenko-Ehrenfest beam theory. It is no exaggeration that the Timoshenko-Ehrenfest beam theory has featured in literally thousands of papers in the literature. However, it is well-known that one of the critical assumptions associated with the Timoshenko-Ehrenfest beam theory is that the theory relies on uniform shear stress distribution through the thickness of the beam cross-section, which does not satisfy the zero shear stress condition on the outer surface of the beam, but nevertheless, the theory takes some partial account of the non-uniform shear stress distribution on an ad-doc basis, by introducing a shear correction factor (also called shape factor). Based on this idea of using the Timoshenko-Ehrenfest beam theory using a rather fictitious shear correction factor [7], numerous publications on the free vibration behaviour of Timoshenko-Ehrenfest beams can be found in the literature. A small sample of the literature, showing significant applications of Timoshenko-Ehrenfest beam theory, can be found in [8-26] in chronological order. A literature survey also shows that there are many investigators who have been seemingly uncomfortable with the Timoshenko-Ehrenfest beam theory because of the assumption of unform shear stress distribution through the cross-section and the subsequent introduction of a somewhat arbitrary shear correction factor on an ad hoc, and perhaps on an improvised basis to rectify the anomaly of non-zero shear stress condition on the outer surface of the beam. Therefore, the search for refined beam theories which dispense with the so-called shear correction or shape factor, continued relentlessly since the emergence of Timoshenko-Ehrenfest beam theory. Notable contributors in this endeavour include Levinson [27], Heyliger and Reddy [28], Kosmatka [29], Huang et al. [30], Nolde et al. [31], Xie et al. [32], Simsek and Kocaturk [33], amongst others, who have used higher order shear deformation theories based on the mathematical theory of elasticity. Carrera et al. [34] made an objective assessment of several refined beam theories including the first author's own theory, called the Carrera Unified Formulation (CUF). The authors of [34] drew many useful conclusions, evaluating each theory on its intrinsic merit, and highlighting each theory's suitability, advantages and disadvantages in different applications. However, the literature on the application of the dynamic stiffness method in conjunction with higher order shear deformation theory for free vibration analysis of beam is scarce with only a couple of research papers appears to have been published in the open literature [35, 36]. The purpose of this paper is to redress this imbalance by developing a new dynamic stiffness theory for beams by using higher order shear deformation theory and extending the earlier research significantly. Some of the errors in the published literature are also rectified. One of the main contributions made in this paper is the application of higher order shear deformation theory for beams to free vibration analysis of frameworks. This is against the background that earlier research was predominantly confined to individual beams rather than frameworks. It should be noted that in recent years, the developments of advanced beam theories have taken numerous turns, particularly when dealing with composite, functionally graded, cracked, micro and nano beams [37-45].

As stated by many of the above investigators, one of the great advantages of using a higher order shear deformation theory in free vibration analysis of beams or frameworks is that it dispenses with the so-called shear correction factor generally adopted in the Timoshenko-Ehrenfest beam formulation to account for the non-uniform shear stress distribution through the thickness of the beam cross-section. A higher order shear deformation theory overcomes this limitation. With this pretext, it should be noted that when carrying out the free vibration analysis of structures, the dynamic stiffness method (DSM) which is called an "exact" method is a powerful alternative to the conventional finite element method (FEM) and other methods. Publications relating to the application of the dynamic stiffness method to solve the beam vibration problem very accurately, using HSDT are indeed scarce. Furthermore, most of the published literature deals with the free vibration behaviour of individual beams using higher order shear deformation theory, but an extension of the theory for applications to frameworks is an open area of research, apparently not undertaken by investigators earlier. This paper is intended to fill this gap in the literature by developing the dynamic stiffness matrix of a beam using a higher order shear deformation theory and then applying it to individual beams as well as frameworks. Advantages of the DSM and its superior modelling capability over FEM and other methods when carrying out free vibration analysis of structures are well known, and there are some survey papers on the subject [46-49]. The DSM is essentially based on the exact solution of the governing differential equation of a structural element when it is undergoing free natural vibration. There are, however, many similarities between FEM and DSM. Both methods are based on the concept of shape functions and nodes of a structure. Notably, DSM uses the frequency-dependent exact shape functions obtained from the solution of the governing differential equation as opposed to the frequency-independent assumed shape functions used in FEM. The procedure to assemble properties of individual structural elements to form the overall matrix is essentially the same. However, there are some significant differences between FEM and DSM. For instance, when solving free vibration problems, the mass and stiffness matrices of individual elements are assembled separately in FEM to form the overall mass and stiffness matrices of the final structure. By contrast, in DSM, there is only one frequency-dependent matrix called the dynamic stiffness matrix containing both the mass and stiffness properties of the element, which is assembled to form the overall dynamic stiffness matrix of the final structure. The other striking feature which distinguishes the two methods is the solution technique for the eigenvalue problem yielding the natural frequencies of a structure. FEM generally leads to a linear eigenvalue problem whereas the DSM leads to a non-linear eigenvalue problem generally solved using the Wittrick-Williams algorithm [50]. As all the assumptions made in DSM are within the limits of the governing differential equations, the results from DSM are usually designated as exact and they are independent of the number of elements used in the analysis. Thus, unlike FEM, further discretization of a structure in DSM is not needed unless there is a change in the geometry or material properties. For instance, a single structural element can be used in DSM to compute any number of natural frequencies of a beam or a plate to any desired accuracy, which of course, is impossible in FEM. Basically, DSM accounts for an infinite number of degrees of freedom of a freely vibrating structure whereas FEM being restricted to a selected number of degrees of freedom at the nodes, does not. For standard structures like beams and plates, DSM gives the same results as the classical theories based on governing differential equations. A secondary purpose of this paper is to assess the accuracy and reliability of existing methods in free vibration analysis of beams and frameworks, essentially by comparison with DSM.

The paper is organised as follows. Following this section on Introduction. Section 2 provides the underlying theory of the paper with subsection 2.1 focusing on the derivation of the governing differential equation of the beam using higher order shear deformation theory. Starting from the choice of the displacement field, the potential and kinetic energies of the beam are formulated, and Hamilton's principle is applied to derive the governing differential equations and associated natural boundary conditions, when the beam is undergoing free vibration. Following this, in subsection 2.2, the differential equations are solved in an exact sense to obtain the expressions for axial displacement, flexural displacement, bending rotation and the first derivative of the flexural displacement. The expressions for shear force, bending moment and the higher-order moment are obtained from the natural boundary conditions resulting from the Hamiltonian formulation. Then in subsection 2.3, the dynamic stiffness matrix is developed by relating the force vector comprising shear force, bending moment and the higher-order moment to the displacement vector comprising flexural displacement, bending rotation and the first derivative of the flexural displacement. In Section 3, the application aspects of the dynamic stiffness matrix are briefly covered, explaining how the dynamic stiffness matrix in axial motion can be incorporated into the derived dynamic stiffness matrix in flexural motion. The use of the transformation matrix is outlined to enable free vibration analysis of frameworks to be made. Also, the solution technique for the free vibration analysis is briefly mentioned by referring to the Wittrick-Williams algorithm. Section 4 deals with numerical results and discussion and finally, conclusions are drawn in Section 5.

2. THEORY

In a Cartesian coordinate system, Fig. 1 shows a rectangular cross-section beam of length *L*, width *b* and height or depth *h*, respectively, as shown, so that the area *A* and the second moment of area *I* of the beam cross-section are respectively, *bh* and $bh^3/12$, respectively. The flexural displacement is assumed to take place in the *YZ* plane with the *Y*-axis coinciding with the centroidal axis of the beam. If the Young's modulus and the density of the beam material are *E* and ρ, respectively, the flexural rigidity and the mass per unit length of the beam are *EI* and ρA, respectively. Based on these beam parameters, and using linear small deflection assumption, the governing differential equations of motion of the beam in free vibration using higher order shear deformation theory are derived as follows.

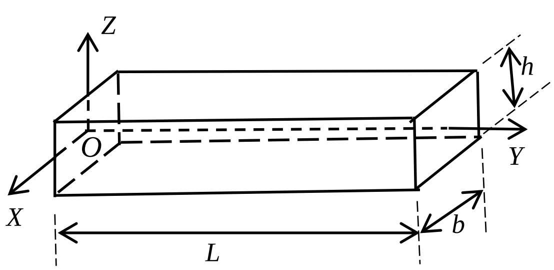

Fig. 1 Beam coordinate system and notation.

2.1 Derivation of the governing differential equations

Referring to Fig. 1, the displacement field for the higher order shear deformation theory for the beam can be written as [27, 28, 35]

$$v = z\left[\theta - \frac{4}{3}\left(\frac{z}{h}\right)^2(\theta + w')\right] \quad (1)$$

where *v* and *w* are the displacement of the beam centreline (or the neutral axis) in the *Y* and *Z*-directions, at a distance *y* from the origin, θ is the bending rotation, i.e., rotation of a normal to the axis of the beam, and a prime represents partial differentiation with respect to *y*.

Using Eq. (1), the normal strain ε, and the shearing strain γ, at a point (*y*, *z*) on the cross-section are given by

$$\varepsilon = \frac{\partial v}{\partial y} = z\left\{\theta' - \frac{4}{3}\left(\frac{z}{h}\right)^2(\theta' + w'')\right\} \quad (2)$$

$$\gamma = \frac{\partial v}{\partial z} + \frac{\partial w}{\partial y} = (\theta + w')\left(1 - \frac{4z^2}{h^2}\right) \quad (3)$$

The potential or strain energy *U* of the beam can then be written as

$$U = \frac{1}{2}\iiint_V \sigma\varepsilon dxdydz + \frac{1}{2}\iiint_V \tau\gamma dxdydz \quad (4)$$

Noting that $\sigma = E\varepsilon$ and $\tau = G\gamma$, the variation δU of the potential energy *U* of Eq. (4) becomes

$$\delta U = \iiint_V E\varepsilon\delta\varepsilon dxdydz + \iiint_V G\gamma\delta\gamma dxdydz \quad (5)$$

With the help of Eqs. (2) and (3), $\delta\varepsilon$ and $\delta\gamma$ can be written as

$$\delta\varepsilon = z\left\{\delta\theta' - \frac{4z^2}{3h^2}(\delta\theta' + \delta w'')\right\} \quad (6)$$

$$\delta\gamma = (\delta\theta + \delta w')\left(1 - \frac{4z^2}{h^2}\right) \quad (7)$$

Substituting Eqs. (6) and (7) into Eq. (5) and noting that the triple integral reduces to a single integral along the length coordinate when integrated over the uniform rectangular area of cross-section of the beam, we obtain

$$\delta U = EI\int_0^L\left[\theta'\delta\theta' - \frac{1}{5}\{(\theta' + w'')\delta\theta' + \theta'(\delta\theta' + \delta w'')\} + \frac{1}{21}(\theta' + w'')(\delta\theta' + \delta w'')\right]dy + \frac{8}{15}GA\int_0^L(\theta + w')(\delta\theta + \delta w')dy \quad (8)$$

The kinetic energy *T* of the beam shown in Fig. 1 is given by [28]

$$T = \frac{1}{2}\iiint_V (\dot{v}^2 + \dot{w}^2)\, dxdydz \quad (9)$$

where an over dot denotes partial differentiation with respect to time *t*.

From Eq. 1, the partial time derivative of *v*, i.e., the $\dot{v}$ term of equation (9) is given by

$$\dot{v} = z\left\{\dot{\theta} - \frac{4z^2}{3h^2}(\dot{\theta} + \dot{w}')\right\} \quad (10)$$

Substituting Eq. (10) into Eq. (9) and noting that its triple integral reduces to a single integral along the length coordinate for a uniform beam such as the one shown in Fig. 1of rectangular cross-section with area *A*, we obtain

$$T = \frac{1}{2}\rho A \int_0^L \dot{w}^2 dy + \frac{1}{2}\rho I \int_0^L \frac{68}{105}\dot{\theta}^2 dy - \frac{1}{2}\rho I \int_0^L \frac{32}{105}\dot{\theta}\dot{w}' dy + \frac{1}{2}\rho I \int_0^L \frac{1}{21}\dot{w}'^2 dy \quad (11)$$

The variation of the kinetic energy δT is thus given by

$$\delta T = \rho A \int_0^L \dot{w}\delta\dot{w}\, dy + \rho I \int_0^L \frac{68}{105}\dot{\theta}\,\delta\dot{\theta} dy - \rho I \int_0^L \frac{16}{105}\dot{\theta}\delta\dot{w}' dy - \rho I \int_0^L \frac{16}{105}\dot{w}'\delta\dot{\theta}\, dy + \rho I \int_0^L \frac{1}{21}\dot{w}'\delta\dot{w}' dy \quad (12)$$

Hamilton's principle states

$$\delta \int_{t_1}^{t_2} (T - V)\, dt = 0 \quad (13)$$

or,

$$\int_{t_1}^{t_2} \delta T dt - \int_{t_1}^{t_2} \delta V dt = 0 \quad (14)$$

where t_1 and t_2 are the time interval of the dynamic trajectory, and δ is the usual variational operator.

The governing differential equations of motion of the beam in free vibration are now derived by substituting δT and δV from Eqs. (12) and (8) into Eq. (14), and then using the δ operator and next integrating by parts, and finally collecting terms. In an earlier publication, the entire procedure to generate the governing differential equations of motion and natural boundary conditions for bar or beam type structures using Hamilton's principle, was automated by Banerjee et al. [51] through the application of symbolic computation. In this way, the governing differential equations of the beam and the natural boundary conditions giving expressions for the shear force (S), bending moment (M) and higher order moment ($\bar{M}$), using higher order shear deformation theory are obtained as follows.

Governing Differential Equations:

$$-\rho A\ddot{w} + \frac{1}{21}\rho I\ddot{w}'' - \frac{16}{105}\rho I\ddot{\theta}' - \frac{1}{21}EIw'''' + \frac{16}{105}EI\theta''' + \frac{8}{15}GAw'' + \frac{8}{15}GA\theta' = 0 \quad (15)$$

$$-\frac{68}{105}\rho I\ddot{\theta} + \frac{16}{105}\rho I\ddot{w}' + \frac{68}{105}EI\theta'' - \frac{16}{105}EIw''' - \frac{8}{15}GA\theta - \frac{8}{15}GAw' = 0 \quad (16)$$

Natural Boundary Conditions:

Shear Force: $S = \frac{1}{21}EIw''' - \frac{16}{105}EI\theta'' - \frac{8}{15}GAw' - \frac{8}{15}GA\theta + \frac{16}{105}\rho I\ddot{\theta} - \frac{1}{21}\rho I\ddot{w}'$ (17)

Bending Moment: $M = \frac{16}{105}EIw'' - \frac{68}{105}EI\theta'$ (18)

Higher Order Moment: $\bar{M} = \frac{16}{105}EI\theta' - \frac{1}{21}EIw''$ (19)

Note that the in the last term of Eq. (18) of [35], there is a typographical sign error in that $\frac{68}{105}AI\rho^2\omega^4$ should be $-\frac{68}{105}AI\rho^2\omega^4$. Also, the expressions for bending moment M and M_h in Eqs. (22) and (23) of [35] should be interchanged. It should be also noted that if the nonlinear terms of [28] are dropped, the governing differential equations and the natural boundary conditions given by Eqs. (15)-(19) above, agree with those given in [28] except that there are some typographical errors in [28] as follows. In the fourth term of Eq. (5) in [28], $-\frac{16}{105}EI$ should be $-\frac{1}{5}EI$ and in the essential boundary conditions for w in Eq. (7), the term $-\frac{1}{21}EI\frac{\partial^2 w}{\partial x^2}$ should be $-\frac{1}{21}EI\frac{\partial^3 w}{\partial x^3}$ and the minus sign in front of ρI should be a plus sign.

2.2 Solution of the Governing Differential Equation

For harmonic oscillation with circular or angular frequency ω rad/s, $w(y, t)$ and $\theta(y, t)$ of Eqs. (15)-(19) can be expressed as

$$w(y,t) = W(y)e^{i\omega t}; \quad \theta(y,t) = \Theta e^{i\omega t} \quad (20)$$

Substituting Eq. (20) into Eqs. (15) and (16) and introducing the non-dimensional length parameter ξ where $\xi = x/L$, gives the following two ordinary differential equations

$$\left\{-\frac{1}{21}EID^4 - \left(\frac{1}{21}\rho I\omega^2 L^2 - \frac{8}{15}GAL^2\right)D^2 + \rho A\omega^2 L^4\right\}W + \left\{\frac{16}{105}EILD^3 + \left(\frac{16}{105}\rho I\omega^2 + \frac{8}{15}GA\right)L^3 D\right\}\Theta = 0 \quad (21)$$

$$\left\{-\frac{16}{105}EID^3 - \left(\frac{16}{105}\rho I\omega^2 L^2 + \frac{8}{15}GAL^2\right)D\right\}W + \left\{\frac{68}{105}EILD^2 + \left(\frac{68}{105}\rho I\omega^2 - \frac{8}{15}GA\right)L^3\right\}\Theta = 0 \quad (22)$$

where

$$D = \frac{d}{d\xi} \quad (23)$$

Eqs. (21) and (22) in which the shear modulus (or the modulus of rigidity) G for isotropic material can be replaced by $\frac{E}{2(1+\nu)}$, ν being the Poisson's ratio, and then they can be combined into a 6th order ordinary differential equation which is identically satisfied by both W and Θ as follows.

$$(D^6 + C_1 D^4 + C_2 D^2 + C_3)H = 0 \quad (24)$$

with

$$H = W \text{ or } \Theta \quad (25)$$

where

$$C_1 = 4b^2r^4(1+\nu) - 70 \quad (26)$$
$$C_2 = 2b^2r^2(1+\nu)(b^2r^4 - 85) - 70b^2r^2 \quad (27)$$
$$C_3 = 70b^2 - 170b^4r^4(1+\nu) \quad (28)$$

with

$$b^2 = \frac{\rho A \omega^2 L^4}{EI}; \quad r^2 = \frac{I}{AL^2} \tag{29}$$

2.2 Solution of the Governing Differential Equations

The solution of the differential equation (Eq. (24)) can be sought in the form

$$W = e^{\lambda\xi} \tag{30}$$

Substituting Eq. (30) into Eq. (24) yields the auxiliary (or characteristic) equation as

$$\lambda^6 + C_1\lambda^4 + C_2\lambda^2 + C_3 = 0 \tag{31}$$

The sixth order polynomial equation above can be expressed as a cubic equation to give

$$\mu^3 + C_1\mu^2 + C_2\mu + C_3 = 0 \tag{32}$$

where

$$\mu = \pm\sqrt{\lambda} \tag{33}$$

The three roots μ (and hence the six roots λ) can now be determined using standard root finding procedures [52].

Thus, the solutions for W and Θ (which are both denoted by H, see Eq. (25)) can be written as

$$W = \sum_{j=1}^{6} A_j\, e^{\lambda_j\xi} \tag{34}$$

$$\Theta = \sum_{j=1}^{6} B_j\, e^{\lambda_j\xi} \tag{35}$$

where λ_j (j= 1; 2; . . . ; 6) are the six roots of Eq. (31) and A_j and B_j are two different sets of six constants.

By substituting Eqs. (34) and (35) into Eq. (21) and using Eq. (29), it can be shown that the constants A_j and B_j are related as follows.

$$B_j = (\alpha_j/L)A_j \tag{36}$$

where

$$\alpha_j = \frac{5(1+\nu)r^2\lambda_j^4 + \{5b^2r^4(1+\nu) - 28\}\lambda_j^2 - 105(1+\nu)b^2r^2}{16(1+\nu)r^2\lambda_j^3 + \{16(1+\nu)b^2r^4 + 28\}\lambda_j} \tag{37}$$

Using Eq. (34), the first derivative W' of the flexural displacement is given by

$$W' = \sum_{j=1}^{6} \lambda_j A_j\, e^{\lambda_j\xi} \tag{38}$$

Now, with the help of Eqs. (17)-(19), and substituting Eq. (29), the expression for the shear force S, bending moment M, and higher order moment $\bar{M}$ are now given by

$$S = \sum_{j=1}^{6} f_j A_j\, e^{\lambda_j\xi} \tag{39}$$

$$M = \sum_{j=1}^{6} g_j A_j\, e^{\lambda_j\xi} \tag{40}$$

$$\bar{M} = \sum_{j=1}^{6} -h_j A_j\, e^{\lambda_j\xi} \tag{41}$$

where

$$f_j = \frac{EI}{105L^3}\left[5\lambda_j^3 - \lambda_j\left\{\frac{56}{2(1+\nu)r^2} - 5b^2r^2\right\} - 16\alpha_j\lambda_j^2 - \left\{\frac{56}{2(1+\nu)r^2} + 16b^2r^2\right\}\alpha_j\right] \tag{42}$$

$$g_j = \frac{EI}{105L^2}\left(16\lambda_j^2 - 68\alpha_j\lambda_j\right) \tag{43}$$

$$h_j = \frac{EI}{105L^2}\left(5\lambda_j^2 - 16\alpha_j\lambda_j\right) \tag{44}$$

2.3 Dynamic Stiffness Matrix Formulation

By relating the amplitudes of forces and moments given by Eqs. (39)-(41) to the amplitudes of displacements and rotations given by Eqs. (34), (35) and (38), the dynamic stiffness matrix is now formulated. This is achieved by applying the boundary or end conditions of the beam.

Referring to Fig. 2, the boundary or end conditions for displacements and rotations are

At end 1, y=0 (ξ=0): W=W_1, Θ=Θ_1 and $W' = W_1'$ (45)

At end 2, y=L (ξ=1): W=W_2, Θ=Θ_2 and $W' = W_2'$ (46)

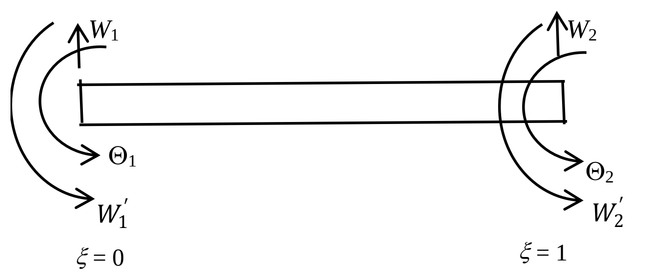

Fig. 2. Boundary or end conditions for displacements

Substituting Eqs. (45) and (46) into Eqs. (34), (35) and (38) gives the following matrix relationship

$$\begin{bmatrix} W_1 \\ \Theta_1 \\ W_1' \\ W_2 \\ \Theta_2 \\ W_2' \end{bmatrix} = \begin{bmatrix} 1 & 1 & 1 & 1 & 1 & 1 \\ \frac{\alpha_1}{L} & \frac{\alpha_2}{L} & \frac{\alpha_3}{L} & \frac{\alpha_4}{L} & \frac{\alpha_5}{L} & \frac{\alpha_6}{L} \\ \frac{\lambda_1}{L} & \frac{\lambda_2}{L} & \frac{\lambda_3}{L} & \frac{\lambda_4}{L} & \frac{\lambda_5}{L} & \frac{\lambda_6}{L} \\ e^{\lambda_1} & e^{\lambda_2} & e^{\lambda_3} & e^{\lambda_4} & e^{\lambda_5} & e^{\lambda_6} \\ \frac{\alpha_1 e^{\lambda_1}}{L} & \frac{\alpha_2 e^{\lambda_2}}{L} & \frac{\alpha_3 e^{\lambda_3}}{L} & \frac{\alpha_4 e^{\lambda_4}}{L} & \frac{\alpha_5 e^{\lambda_5}}{L} & \frac{\alpha_6 e^{\lambda_6}}{L} \\ \frac{\lambda_1 e^{\lambda_1}}{L} & \frac{\lambda_2 e^{\lambda_2}}{L} & \frac{\lambda_3 e^{\lambda_3}}{L} & \frac{\lambda_4 e^{\lambda_4}}{L} & \frac{\lambda_5 e^{\lambda_5}}{L} & \frac{\lambda_6 e^{\lambda_6}}{L} \end{bmatrix} \begin{bmatrix} A_1 \\ A_2 \\ A_3 \\ A_4 \\ A_5 \\ A_6 \end{bmatrix} \tag{47}$$

or,

$$\boldsymbol{\delta} = \mathbf{QA} \tag{48}$$

where $\boldsymbol{\delta}$ is the displacement vector, **A** is the constant vector and **Q** is the square 6x6 matrix in Eq. (47).

Now, referring to Fig. 3, the boundary or end conditions for shear forces, and moments are

At end 1, $y=0$ ($\xi=0$): $S=S_1$, $M=M_1$ and $\bar{M} = \bar{M}_1$ (49)

At end 2, $y=L$ ($\xi=1$): $S=-S_2$, $M=-M_2$ and $\bar{M} = -\bar{M}_2$ (50)

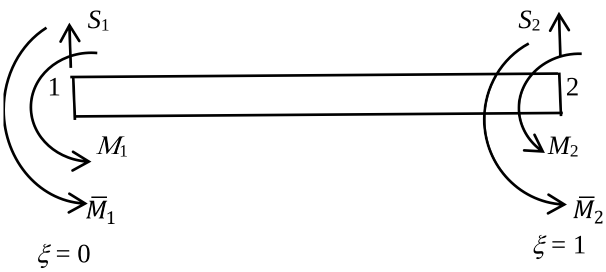

Fig. 3. Boundary or end conditions for forces and moments

Substituting Eqs. (49) and (50) into Eqs. (39)-(41) gives the following matrix relationship

$$\begin{bmatrix} S_1 \\ \mathrm{M}_1 \\ \bar{M}_1 \\ S_2 \\ \mathrm{M}_2 \\ \bar{M}_2 \end{bmatrix} = \begin{bmatrix} f_1 & f_2 & f_3 & f_4 & f_5 & f_6 \\ g_1 & g_2 & g_3 & g_4 & g_5 & g_6 \\ -h_1 & -h_2 & -h_3 & -h_4 & -h_5 & -h_6 \\ -f_1 e^{\lambda_1} & -f_2 e^{\lambda_2} & -f_3 e^{\lambda_3} & -f_4 e^{\lambda_4} & -f_5 e^{\lambda_5} & -f_6 e^{\lambda_6} \\ -g_1 e^{\lambda_1} & -g_2 e^{\lambda_2} & -g_3 e^{\lambda_3} & -g_4 e^{\lambda_4} & -g e^{\lambda_5} & -g_6 e^{\lambda_6} \\ h_1 e^{\lambda_1} & h_2 e^{\lambda_2} & h_3 e^{\lambda_3} & h_4 e^{\lambda_4} & h_5 e^{\lambda_5} & h_6 e^{\lambda_6} \end{bmatrix} \begin{bmatrix} A_1 \\ A_2 \\ A_3 \\ A_4 \\ A_5 \\ A_6 \end{bmatrix} \quad (51)$$

or,

$$\mathbf{f} = \mathbf{RA} \quad (52)$$

The constant vector, **A** can now be eliminated from Eqs. (48) and (52) to give

$$\mathbf{f} = \mathbf{RQ}^{-1}\boldsymbol{\delta} = \mathbf{K}\boldsymbol{\delta} \quad (53)$$

where

$$\mathbf{K} = \mathbf{RQ}^{-1} \quad (54)$$

is the required dynamic stiffness matrix.

Thus, the force-displacement relationship at the nodes of a beam using higher order shear deformation theory is given by

$$\begin{bmatrix} S_1 \\ M_1 \\ \bar{M}_1 \\ S_2 \\ M_2 \\ \bar{M}_2 \end{bmatrix} = \begin{bmatrix} k_{11} & k_{12} & k_{13} & k_{14} & k_{15} & k_{16} \\ k_{12} & k_{22} & k_{23} & k_{24} & k_{25} & k_{26} \\ k_{13} & k_{23} & k_{33} & k_{34} & k_{35} & k_{36} \\ k_{14} & k_{24} & k_{34} & k_{44} & k_{45} & k_{46} \\ k_{15} & k_{25} & k_{35} & k_{45} & k_{55} & k_{56} \\ k_{16} & k_{26} & k_{36} & k_{46} & k_{56} & k_{66} \end{bmatrix} \begin{bmatrix} W_1 \\ \Theta_1 \\ W_1' \\ W_2 \\ \Theta_2 \\ W_2' \end{bmatrix} = \begin{bmatrix} \mathbf{k_{11}} & \mathbf{k_{12}} \\ \mathbf{k_{21}} & \mathbf{k_{22}} \end{bmatrix} \begin{bmatrix} W_1 \\ \Theta_1 \\ W_1' \\ W_2 \\ \Theta_2 \\ W_2' \end{bmatrix} \quad (55)$$

where $\mathbf{k}_{11}$, $\mathbf{k}_{12}$, $\mathbf{k}_{21}$ and $\mathbf{k}_{22}$ are 3×3 submatrices and $\mathbf{k}_{21}$ is the transpose of $\mathbf{k}_{12}$.

When computing the dynamic stiffness matrix **K** of (54), it should be noted that the roots λ and μ of Eqs. (31) and (32) can be complex and therefore, the elements of matrices **Q** and **R** of Eqs. (48) and (52) can also be complex. Therefore, the matrix inversion and multiplication steps of Eq. (54) must be carried out using complex arithmetic. The resulting dynamic stiffness matrix **K** will, of course, be symmetric and real, with imaginary parts of each element being zero. Now the dynamic stiffness matrix in axial or longitudinal motion which is readily available in the literature [53, 54, 55] and is uncoupled from flexural motion, can be incorporated into the dynamic stiffness matrix **K** in flexural motion derived above so that the free vibration analysis of frames can be made. The force-displacement relationship using the dynamic stiffness matrix of a beam element in axial or longitudinal vibration with the amplitudes of axial forces and displacements at nodes 1 and 2, being F_1, F_2 and V_1, V_2, respectively is given by [53, 54, 55]

$$\begin{bmatrix} F_1 \\ F_2 \end{bmatrix} = \frac{EA}{L} \begin{bmatrix} a_1 & a_2 \\ a_2 & a_1 \end{bmatrix} \begin{bmatrix} V_1 \\ V_2 \end{bmatrix} \quad (56)$$

where

$$a_1 = \frac{EA}{L} \bar{\mu} \cot \bar{\mu}; \quad a_2 = -\bar{\mu} \operatorname{cosec} \bar{\mu} \quad (57)$$

with

$$\bar{\mu} = \omega L \sqrt{\frac{\rho A}{EA}} \quad (58)$$

The dynamic stiffness matrix in axial motion given by Eq. (56) when incorporated into the dynamic stiffness matrix in flexural motion given by Eq. (55), leads to

$$\begin{bmatrix} F_1 \\ S_1 \\ M_1 \\ \bar{M}_1 \\ F_2 \\ S_2 \\ M_2 \\ \bar{M}_2 \end{bmatrix} = \begin{bmatrix} a_1 & 0 & 0 & 0 & e_1 & 0 & 0 & 0 \\ 0 & k_{11} & k_{12} & k_{13} & 0 & k_{14} & k_{15} & k_{16} \\ 0 & k_{12} & k_{22} & k_{23} & 0 & k_{24} & k_{25} & k_{26} \\ 0 & k_{13} & k_{23} & k_{33} & 0 & k_{34} & k_{35} & k_{36} \\ e_1 & 0 & 0 & 0 & a_1 & 0 & 0 & 0 \\ 0 & k_{14} & k_{24} & k_{34} & 0 & k_{44} & k_{45} & k_{46} \\ 0 & k_{15} & k_{25} & k_{35} & 0 & k_{45} & k_{55} & k_{56} \\ 0 & k_{16} & k_{26} & k_{36} & 0 & k_{46} & k_{56} & k_{66} \end{bmatrix} \begin{bmatrix} V_1 \\ W_1 \\ \Theta_1 \\ W_1' \\ V_2 \\ W_2 \\ \Theta_2 \\ W_2^1 \end{bmatrix} = \begin{bmatrix} \mathbf{K}_{11} & \mathbf{K}_{12} \\ \mathbf{K}_{21} & \mathbf{K}_{22} \end{bmatrix} \begin{bmatrix} V_1 \\ W_1 \\ \Theta_1 \\ W_1' \\ V_2 \\ W_2 \\ \Theta_2 \\ W_2^1 \end{bmatrix} \quad (59)$$

where

$$\mathbf{K}_{11} = \begin{bmatrix} a_1 & 0 & 0 & 0 \\ 0 & k_{11} & k_{12} & k_{13} \\ 0 & k_{12} & k_{22} & k_{23} \\ 0 & k_{13} & k_{23} & k_{33} \end{bmatrix}; \ \mathbf{K}_{12} = \begin{bmatrix} e_1 & 0 & 0 & 0 \\ 0 & k_{14} & k_{15} & k_{16} \\ 0 & k_{15} & k_{25} & k_{26} \\ 0 & k_{34} & k_{35} & k_{36} \end{bmatrix}; \mathbf{K}_{22} = \begin{bmatrix} a_1 & 0 & 0 & 0 \\ 0 & k_{44} & k_{45} & k_{46} \\ 0 & k_{45} & k_{55} & k_{56} \\ 0 & k_{46} & k_{56} & k_{66} \end{bmatrix} \quad (60)$$

and $\mathbf{K}_{21}$ can be obtained by taking the transpose of $\mathbf{K}_{12}$.

3. APPLICATION OF THE THEORY

The dynamic stiffness matrix developed above, can now be used to compute the natural frequencies and mode shapes of either a single beam or an assembly of beams, e.g., a framework. However, to apply the theory to a framework, the dynamic stiffness matrix of Eqs. (59) and (60), developed for an individual beam element in its local coordinates must be transformed into global (or datum) coordinates.

Figure 4 shows the local (YZ) and global ($\bar{Y}\bar{Z}$) coordinate systems of a beam element with the local Y-axis making an angle ϕ with the global $\bar{Y}$-axis (measured positive anticlockwise). The transformation matrix $\mathbf{T}$ to transform the submatrices $\mathbf{K}_{11}$, $\mathbf{K}_{12}$, $\mathbf{K}_{21}$ and $\mathbf{K}_{22}$ of Eqs. (59) and (60) from local coordinates to global (or datum coordinates) is given by [54, 55]

$$\mathbf{T} = \begin{bmatrix} \cos\phi & \sin\phi & 0 & 0 \\ -\sin\phi & \cos\phi & 0 & 0 \\ 0 & 0 & 1 & 0 \\ 0 & 0 & 0 & 1 \end{bmatrix} \tag{61}$$

The transformed stiffness matrices $\bar{\mathbf{K}}_{11}$, $\bar{\mathbf{K}}_{12}$ and $\bar{\mathbf{K}}_{22}$, in global coordinates are given by [54, 55]

$$\bar{\mathbf{K}}_{11} = \mathbf{T}^{\mathrm{T}}\mathbf{K}_{11}\mathbf{T};\ \bar{\mathbf{K}}_{12} = \mathbf{T}^{\mathrm{T}}\mathbf{K}_{12}\mathbf{T};\ \bar{\mathbf{K}}_{22} = \mathbf{T}^{\mathrm{T}}\mathbf{K}_{22}\mathbf{T} \tag{62}$$

where the upper suffix of T denotes a transpose and $\bar{\mathbf{K}}_{21}$ is $\bar{\mathbf{K}}_{12}^{\mathrm{T}}$.

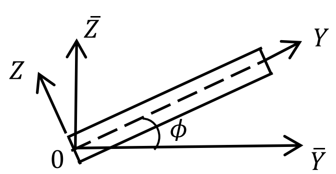

Fig. 4. Local and Global Coordinate System of a Beam Element

The transformed stiffness matrices $\bar{\mathbf{K}}_{11}$, $\bar{\mathbf{K}}_{12}$ $\bar{\mathbf{K}}_{21}$ and $\bar{\mathbf{K}}_{22}$ can now be used to form the overall dynamic stiffness matrix of a frame in a global or datum coordinate system.

Once the overall global dynamic stiffness matrix $\bar{\mathbf{K}}$ of a frame is formed, the Wittrick-Williams algorithm [46-50] can be used as a solution technique to compute the natural frequencies and subsequently recover the mode shapes of the frame.

4. RESULTS AND DISCUSSION

The theory developed above is now applied for free vibration analysis of five illustrative examples of different types. The first illustrative example is taken from Carrera et al [34] which is that of a cantilever beam with solid rectangular cross-section. The authors of [34] have used Carrera Unified Formulation (CUF), Timoshenko-Ehrenfest and Bernoulli-Euler beam theories and a 3D finite element analysis and made comparative assessments of results. The width (b) and depth or height (h) of the beam cross-section are 1m and 0.1m, respectively and the length L of the beam is 10m, as given in [34]. The material properties of the beam are that of aluminum with Young's modulus E = 69 MPa, density ρ = 2700 kg/m^3 and Poisson's ratio ν=0.33 [34]. The first four natural frequencies f_i (i = 1, 2 , 3 and 4) in Hz of the cantilever beam were computed using the present theory and the results are shown in Table 1 alongside the results reported in [34]. The results from the present theory are in excellent agreement with the CUF theory, Timoshenko-Ehrenfest theory and 3D finite element results, the discrepancy being less than 1.5%. Note that the results for the Timoshenko-Ehrenfest beam theory shown in Table 1 were computed using the exact frequency dependent mass and stiffness matrices derived by the current author in a recently published paper [53] as well by using the published program of [55]. The shear correction or shape factor used in the analysis was set to 5/6. Also, it should also be noted that that unlike the 1st, 2nd and 4th natural frequencies which corresponds to in-plane free vibration of the beam in the YZ-plane (see Fig. 1), the 3rd natural frequency corresponds to an out of plane natural frequency for which the free vibratory motion takes place in the XY-plane (see Fig. 1). The mode shapes for the first four natural frequencies using the higher order shear deformation theory developed in this paper are illustrated in Fig. 5, showing flexural displacement W, bending rotation Θ and the first derivative of the flexural displacement W' in each mode. From the mode shapes, it may be noted that the bending rotation Θ and the first derivative of the flexural displacement W' in each of the four mode shapes are almost equal and opposite which leads to the assertion that the shearing strain in these modes is almost zero which is in accord with Eq. (3). This is to be expected for a beam [34] of this type which has a slender ratio (length over the radius of gyration) approaching 350, for which the shearing strain is not expected to have any major effect.

Table 1 Natural frequencies of a cantilever beam

Freq. No (i)	Natural frequency f_i (Hz)			
	Present	TEBT [53]	CUF [34]	3D FEM [34]
1	0.8165	0.8165	0.8255	0.8325
2	5.1148	5.1151	5.1702	5.2142
3	8.1014	8.1090	8.1443	8.0181
4	14.310	14.3156	14.4193	14.5998

Table 2 Natural frequencies of a simply-supported beam

Freq. No (i)	Natural frequency ω_i (rad/s)		
	Present	TEBT [24, 53, 55]	BEBT [24]
1	6916.02	6838.83 (1.12%)	7368.07 (6.54%)
2	23949.7	23190.8 (3.17%)	29472.2 (23.1%)
3	40622.3	43443.5 (6.94%)	66312.7 (63.2%)
4	45734.9	64939.2 (42.0%)	117889.1 (158%)

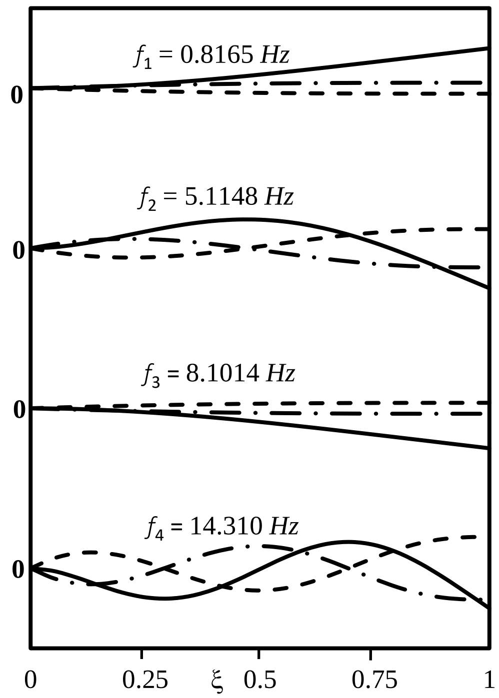

Fig.5 Mode shapes of a cantilever beam using HSDT
——— W; – – – – Θ; — · — · — W'

The second illustrative example is that of a Timoshenko-Ehrenfest beam reported by Chen et al. [24] and Banerjee [53]. The beam material properties are Young's modulus E = 210 GPa, density ρ = 7850 kg/m^3 and Poisson's ratio ν =1/3. The shear modulus G was calculated by relating it to E through the Poisson's ratio ν to give G = 3E/8 [24]. The beam is of rectangular cross-section with width b = 0.02m, depth or height h = 0.08m and it has a length L = 0.4m. The shear correction factor (also known as shape factor) was set to k = 2/3 as used in [24, 53] when computing the results by using the Timoshenko-Ehrenfest beam theory [53, 55]. The Bernoulli-Euler beam theory (BEBT) results were obtained using the published program of Williams and Howson [54]. This example was chosen because unlike the previous example in which the beam had a slenderness ratio of around 350, this example beam has a slenderness ratio of around 17. Thus, there are significant differences between the two examples so that the results can be compared and contrasted to demonstrate the correctness and accuracy of the theory. Table 2 shows the results for the first four in-plane natural frequencies of the beam with simple-supported (S-S) boundary conditions, using the present HSDT theory, Bernoulli-Euler beam theory (BEBT) [54] and the Timoshenko-Ehrenfest beam theory (TEBT) [24, 53, 55]. The percentage differences in results for the first four natural frequencies using the Timoshenko-Ehrenfest beam theory (TEBT) and the Bernoulli-Euler Beam theory (BEBT) as opposed to the present HSDT theory are shown in the parentheses of columns 3 and 4 of the table. For the four natural frequencies quoted, the TEBT results deviate by 1.12%, 3,17%, 6.94% and 42%, respectively whereas for the BEBT results the deviations are by 6.54%, 23.1%, 63.2% and 158%, respectively. Clearly the differences are much larger compared to the previous example due mainly to the low slenderness of the beam.

The third illustrative example is taken from a recently published paper [45] which deals with the free vibration analysis of cracked beams by applying the finite element method based on the Reddy beam theory [28] which in fact is the higher order shear deformation theory used in this paper. This example is chosen because the paper [45] uses the same displacement field as that of the present paper to describe the normal and shear stress and strain distributions of the beam but relies on the finite element method as opposed to the dynamic stiffness method of the present paper. Of course, both methods dispense with the so-called shear correction factor, generally employed in the Timoshenko-Ehrenfest beam theory [5-16]. Although the authors of [45] focused their attention on cracked beams, they, nevertheless, presented results for the degenerate case for the intact beam, i.e. when the crack was absent. The results for the first four natural frequencies for clamped-simply supported boundary condition of the beam using the present theory are shown in Table 3 together with the results reported in [45]. To be consistent with the results given in [45], the non-dimensional frequency parameter $\bar{\lambda}_i$ (i =1, 2, 3, 4) is used, where

$$\bar{\lambda}_i = \sqrt[4]{\frac{\omega^2 \rho A L^4}{EI}} \qquad (63)$$

Results using the Bernoulli-Euler and Timoshenko beam theories were obtained using the published programs of [54] and [55] which are also shown in Table 3 in non-dimensional form. As can be seen, the results from the present theory are in close agreement with those of [45] which applied finite element method but used higher order shear deformation theory based on the same displacement field as the present paper. However, the results from the Timoshenko-Ehrenfest beam theory (TEBT) differed from the present theory by 1.5%, 2.7%, 3.6% and 4.2% in the first four natural frequencies, respectively whereas the corresponding differences using the Bernoulli-Euler beam theory (BEBT) are 7.1%, 16.2%, 26.1% and 35.8%, respectively. As expected, the BEBT which ignores the effects of shear deformation gives relatively large errors in the natural frequencies.

Table 3 Natural frequencies of a clamped-simply supported beam

Freq. No (i)	Non-dimensional natural frequency $\bar{\lambda}_i = \sqrt[4]{\frac{\omega^2 \rho A L^4}{EI}}$			
	Present	Ref [45]	TEBT [55]	BEBT [54]
1	3.6662	3.6710	3.6124	3.9266
2	6.0814	6.0957	5.9185	7.0686
3	8.0990	8.1237	7.8108	10.210
4	9.8313	9.8662	9.4176	13.352

The next example is that of a portal frame shown in Fig. 6. This problem was investigated earlier by Banerjee [56] and Doyle [57], in very different contexts. Each beam member of the portal frame of Fig. 6 is considered here of thin-walled circular cross-section with external and internal diameters 0.25m and 0.24m, respectively so that the thickness of the tubular cross-section is 0.01m. The length L is set to 5m. The material properties used are that of steel with Young's modulus E=200 GPa, and density ρ = 7500 kg/m^3 so that the axial or extensional and flexural rigidities and the mass per unit length are worked out to be EA=1.5708×10^9 N, EI=5.7775×10^6 Nm^2, and ρA= 58.905 kg/m, respectively. The Poisson's ratio is taken to be 1/3. The first six natural frequencies of the portal frame are shown in Table 4 using the present theory as well as the Timoshenko-Ehrenfest [53] and Bernoulli-Euler [54] beam theories. The results using the present theory are close to those of the Timoshenko-Ehrenfest theory, but the Bernoulli-Euler theory caused a small difference with maximum discrepancy of around 2% in the sixth natural frequency. This is expected because the slenderness ratio of each of the frame members is around 80. Doyle [57] quoted the fundamental frequency of the frame, which in current form is 2.649, close to the present theory.

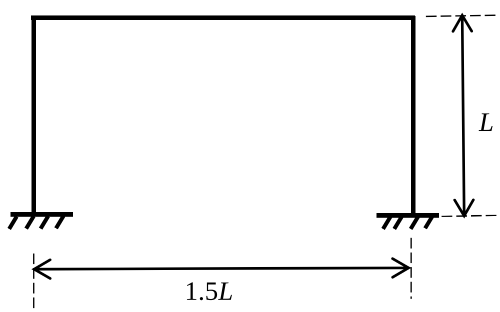

Fig.6 A Portal Frame

Table 4 Natural frequencies of portal frame of Fig. 6

Freq. No (i)	Non-dimensional natural frequency $\bar{\omega}_i = \sqrt{\frac{\omega^2 \rho A L^4}{EI}}$		
	Present	TEBT [55]	BEBT [56]
1	2.6585	2.6583	2.6642
2	6.7844	6.7839	6.8083
3	16.839	16.838	16.948
4	18.924	18.925	19.106
5	25.301	25.297	25.605
6	42.584	42.581	43.220

The final example is a portal frame containing inclined members as shown in Fig. 7. The member properties and the length L are taken to be the same as those of the portal frame in the previous example. The first six natural frequencies of the portal frame computed using the present theory as well as by the Timoshenko-Ehrenfest and Bernoulli-Euler theories, are shown in Table 5. As was the case with the previous portal frame, the results from the present theory are in excellent agreement with those obtained from the Timoshenko-Ehrenfest beam theory (TEBT), but the Bernoulli-Euler beam theory (BEBT) yielded a small difference of around 3% in the sixth natural frequency. The small differences in the results can be attributed to the fact that like the previous example of the portal frame, each member of the portal frame of Fig. 6 has a slenderness ratio more than 80.

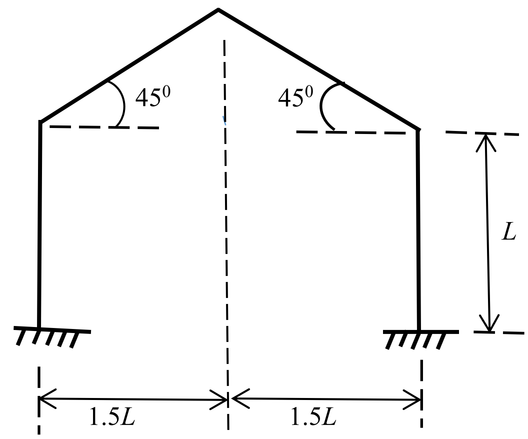

Fig. 7 A portal frame with inclined members

Table 5. Natural frequencies of a portal frame of Fig. 7

Freq. No (i)	Non-dimensional natural frequency $\bar{\omega}_i = \sqrt{\frac{\omega^2 \rho A L^4}{EI}}$		
	Present	TEBT [55]	BEBT [56]
1	2.0733	2.0732	2.0766
2	5.1462	5.1459	5.1560
3	11.678	11.677	11.730
4	14.704	14.703	14.803
5	21.858	21.855	22.099
6	22.863	22.861	23.081

5. CONCLUSIONS

Using higher order shear deformation theory, the dynamic stiffness method is developed for free vibration analysis of beams and frameworks. The unique feature of the dynamic stiffness method in which exact member theory resulting from the solution of the governing differential equations of motion is applied when developing the theory and subsequently obtaining the results. Comparative results for the natural frequencies using Timoshenko-Ehrenfest and Bernoulli-Euler theories are also presented. Representative mode shapes are illustrated. The accuracy and robustness of the theory are demonstrated by numerical results which showed excellent agreement with published results in the literature. The extension of the higher order shear deformation theory for free vibration analysis of frameworks using the dynamic stiffness method is entirely novel and is an important contribution to the literature.

ACKNOWLEDGEMENTS

The author benefitted from an earlier funding from the Engineering and Physical Research Council (EPSRC), UK (Grant Ref: GR/R21875/01) to whom acknowledgement is hereby made. The author also thanks Professor David Kennedy for help given in the development of computer programs needed in this research, and for many insightful comments.

REFERENCES

1. Euler, L., 1744, *De Curvis Elasticis*, Bousquet, Lausanne and Geneva.
2. Bernoulli, D., 1751, "De Vibrationibus et Sono Laminarum Elasticarum", Comment. Acad. Sci. Imp. Petropol., **13**, pp. 105-120.
3. Lord Rayleigh, 2011, *The Theory of Sound*, Vol. 1-2, Cambridge University Press, Cambridge.
4. Searle J.H.C., 1907, "The Effects of Rotatory Inertia on the Vibration of Bars," Philos. Mag., **14**, 35-42, https://doi.org/10.1080/14786440709463660
5. Timoshenko, S.P., 1921, "On the Correction for Shear of the Differential Equation for Transverse Vibrations of Prismatic Bars", Philos. Mag., **41** (245), pp. 744-746 https://doi.org/10.1080/14786442108636264
6. Timoshenko, S.P., 1922, "On the Transverse Vibrations of Bars of Uniform Cross-sections", Philos. Mag., **43** (253), pp. 125-131. https://doi.org/10.1080/14786442208633855
7. Dong, S.B., Alpdogan, C. and Taciroglu, E., 2010, "Much ado about shear correction factors in Timoshenko beam theory", Int. J. Solids Struct., 47, pp. 1651-1665.
8. Traill-Nash, R.W., and Collar, A.R., 1953, "The Effects of Shear Flexibility and Rotatory Inertia on Bending Vibrations of Beams", Q. J. Mech. Appl. Math., 6 (2), pp. 186-222. https://doi.org/10.1093/qjmam/6.2.186
9. Anderson, R.A., 1953, "Flexural Vibrations in Uniform Beams According to Timoshenko Theory", J. Appl. Mech., 20 (4), pp. 504-510. https://doi.org/10.1115/1.4010755
10. Dolph, C.L., 1954, "On the Timoshenko Theory of Transverse Vibration", Q. Appl. Math., 12 (2), pp. 175-187. https://www.jstor.org/stable/43634130
11. Boley, B.A., and Chao, C.C., 1955, "Some Solutions of the Timoshenko Beam Equations", J. Appl. Mech., 22 (4), pp. 579-586. https://doi.org/10.1115/1.4011158
12. Huang, T.C., 1961, "The Effect of Rotary Inertia and of Shear Deformation on the Frequency and Normal Mode Equations of Uniform Beams with Simple End Conditions", J. Appl. Mech., 28 (4), pp. 579-584. https://doi.org/10.1115/1.3641787
13. Nederveen, C.J., and Schwarzl, F.R., 1964, "Correction for Shear and Rotatory Inertia on Flexural Vibration of Beams", Br. J. Appl. Phys., 15 (3), pp. 323-325. https://doi.org/10.1088/0508-3443/15/3/413
14. Carr, J.B., 1970, "The Effect of Shear Flexibility and Rotatory Inertia on the Natural Frequencies of Uniform Beams", Aeronaut. Q., 21 (1), pp. 79-90. https://doi.org/10.1017/S0001925900005242
15. Downs, B., 1976, "Transverse Vibration of a Uniform, Simply Supported Timoshenko Beam without Transverse Deflection", J. Appl. Mech., 43 (4), pp. 671-674. https://doi.org/10.1115/1.3423953
16. Grant, D.A., 1978, "The Effect of Rotary Inertia and Shear Deformation on the Frequency and Normal Mode Equations of Uniform Beams Carrying a Concentrated Moving Mass", J. Sound Vib., 57 (3), pp. 357-365. https://doi.org/10.1016/0022-460X(78)90316-4
17. Levinson, M, and Cooke, D.W., 1982, "On the Two Frequency Spectra of Timoshenko Beams", J. Sound Vib., 84 (3), pp. 319-326. https://doi.org/10.1016/0022-460X(82)90480-1
18. Stephen, N.G., 1982, "The Second Frequency Spectrum of Timoshenko Beams", J. Sound Vib., 80 (4), pp. 578-582. https://doi.org/10.1006/jsvi.1996.0885
19. White, M.W.D., and Heppler, G,R., 1995, "Vibration Modes and Frequencies of Timoshenko Beams with Attached Rigid Bodies", J. Appl. Mech., 62 (1), pp. 193-199. https://doi.org/10.1115/1.2895902
20. Horr, A.M., and Schmidt, L.C. 1995, "Closed-Form Solution for the Timoshenko Beam Theory Using a Computer-Based Mathematical Package", Comput. Struct., 55 (3), pp. 405-412. https://doi.org/10.1016/0045-7949(95)98867-P
21. O'Reilly, O.M., and Turcotte, J.S., 1996, "Another Mode of Vibration in a Timoshenko Beam", J. Sound Vib., 198 (4), pp. 517-521. https://doi.org/10.1006/jsvi.1996.0585
22. Zhou, D., 2001, "Free Vibration of Multi-Span Timoshenko Beams using Static Timoshenko Beam Functions", J. Sound Vib., 241 (4), pp. 725-734. https://doi.org/10.1006/jsvi.2000.3266

23. Antes, H., 2003, “Fundamental Solution and Integral Equations for Timoshenko Beams”, Comput. Struct., 81 (6), pp. 383-396. https://doi.org/10.1016/S0045-7949(02)00452-2

24. Chen G, Qian L, Yin Q. Dynamic analysis of a Timoshenko beam subjected to an accelerating mass using spectral element method. Shock Vib 2014 (5): Paper 768209. http://dx.doi.org/10.1155/2014/768209

25. Elishakoff, I., 2020, “Who Developed the So-Called Timoshenko Beam Theory?”, Math. Mech. Solids, 25 (1), pp. 97-116. https://doi.org/10.1177/1081286519856931

26. Elishakoff, I., 2020, Handbook on Timoshenko-Ehrenfest Beam and Uflyand-Mindlin Plate Theories, World Scientific, Singapore. https://doi.org/10.1142/10890

27. Levinson, M., 1981, “A New Rectangular Beam Theory”, J. Sound Vib.,74 (1), pp. 81-87.

28. Heyliger, P.R., and Reddy, J.N., 1988, “A Higher Order Beam Finite Element for Bending and Vibration Problems”, J. Sound Vib.,126 (2), pp. 309-326.

29. Kosmatka, J.B., 1993, “Transverse Vibrations of Shear-Deformable Beams Using a General Higher Order Theory”, J. Sound Vib.,160 (2), pp. 259-277.

30. Huang, Y., Wu, J.X., Li, X.F., and Yangang L.E., 2013, “Higher-Order Theory for Bending and Vibration of Beams with Circular Cross Section”, J. Eng. Math., 80, pp. 91-104

31. Nolde, E., Pichugin, A.V., and Kaplunov, J., 2018, “An Asymptotic Higher-Order Theory for Rectangular Beams”, Proceed. Royal Soc. A, 474(2214), Paper 20180001. http://doi.org/10.1098/rspa.2018.0001

32. Xie, L., Wang, S., Ding, J., Banerjee, J.R., and Wang, J., 2020, “An Accurate Beam Theory and its First-Order Approximation in Free Vibration Analysis”, J. Sound Vib.,485, Paper 115567.

33. Simsek, M, and Kocaturk, T., 2007, “Free Vibration Analysis of Beams by Using a Third-Order Shear Deformation Theory”, Sadhana, 32(3), pp. 167-179.

34. Carrera, E., Miglioretti, F. and Petrolo, M., 2012 “Computations and evaluations of higher-order theories for free vibration analysis of beams”, J. Sound Vib.,331, pp. 4269-4284.

35. Eisenberger, M., 2003, “Dynamic Stiffness Vibration Analysis Using a High-Order Model”, Int. J. Num. Meth. Eng., 57, pp. 1603-1614. doi: 10.1002/nme.736

36. Li, J., Shi, Z., and Ning, S., 2017, “A Two-Dimensional Consistent Approach for Static and Dynamic Analyses of Uniform Beams”, Eng. Analy. Bound. Element, 82, 1-16.

37. Shi, G., Lam, K.Y., and Tay, T.E., 1998, “On efficient finite element modeling of composite beams and plates using higher-order theories and an accurate composite beam element”, Compos. Struct., 41, pp. 159-165.

38. Civalek, O., Akbas, S.D., Akgöz, B., and Dastjerdi, S., 2021, “Forced Vibration Analysis of Composite Beams Reinforced by Carbon Nanotubes”, Nanomaterials, 11(3): Paper 571

39. Demir, C., and Civalek, O., 2017, “On the Analysis of Microbeams”. Int. J. Eng. Sci., 121, pp. 14-33.

40. Noori, J., Fariborz, S.J., and Vafa, P., 2016, “A Higher-Order Micro-Beam Model with Application to Free Vibration”, Mech. Adv. Material Struct., 23(4), pp. 443-450.

41. Zohra, Z.F., Lemya, H.A., Abderahman, Y., Mustapha, M, Abdelouahed, T., and Djamel, O., 2017, “Free vibration analysis of functionally graded beams using a higher-order shear deformation theory”, Math. Modelling Eng. Problems, 4(1), pp. 7-12. doi: 10.18280/mmep.040102

42. Ghugal, Y.M., and Shimpi, R.P., 2001, “A Review of Refined Shear Deformation Theories for Isotropic and Anisotropic Laminated Beams”, J. Reinf. Plast. Compos., 20, pp. 255-272. doi: 10.1177/073168401772678283

43. Torabi, K., and Dastgerdi, J.N., 2012, “An analytical method for free vibration analysis of Timoshenko beam theory applied to cracked nanobeams using a nonlocal elasticity model”, Thin Solid Films, 520, pp. 6595-6602.

44. Aria, A.I., Friswell, M.I., and Rabczuk, T., 2019, “Thermal vibration analysis of cracked nanobeams embedded in an elastic matrix using finite element analysis”, Compos. Struct., 212, pp. 118-128.

45. Taima, M.S., EI-Sayed, T., Shehab, M.M., Farghaly, S.H., and Hand, R.J., 2023, “Vibration analysis of cracked beam based on Reddy beam theory by finite element method”, J. Vib. Contr., 29(19-20), pp. 4589-4606. doi.org/10.1177/10775463221122122

46. F.W. Williams, W.H. Wittrick, Exact buckling and frequency calculations surveyed, J. Struct. Eng. 109 (1) (1983) 169-187. https://doi.org/10.1061/(ASCE)0733-9445(1983)109:1(169)

47. Williams, F.W., 1993, "Review of exact buckling and frequency calculations with optional multi-level substructuring", Comput. Struct., 48, pp. 547–52.

48. J.R. Banerjee, The dynamic stiffness method: theory, practice and promise, Computational Technology Reviews, Saxe-Coburg Publications 11 (2015) 31-57.

49. J.R. Banerjee, Review of the dynamic stiffness method for free-vibration analysis of beams, Transport. Safety Environ. 1 (2) (2019) 106–116.

50. Wittrick, W.H., and Williams, F.W., 1971, "A General Algorithm for Computing Natural Frequencies of Elastic Structures," Quart. J. Mech. Appl. Math., **24** (3), pp. 263–284. http://dx.doi.org/10.1093/qjmam/24.3.263

51. Banerjee, J.R., Sobey, A.J., Su, H., and Fitch, J.P., 2008, "Use of computer algebra in Hamiltonian calculations", Adv. Eng. Software, 39(6), pp.521-525. https://doi.org/10.1016/j.advengsoft.2007.03.013

52. Pipes, L.A., and Harvill, L.R., 1971, *Applied Mathematics for Engineers*, McGraw-Hill, New York.

53. Banerjee, J.R., 2022, "Free Vibration of Timoshenko–Ehrenfest Beams and Frameworks Using Frequency-Dependent Mass and Stiffness Matrices", J. Vib. Acous., 144(6), pp. 064501-7. doi:10.1115/1.4055133

54. Williams, F.W., and Howson, W.P., 1977, "Compact Computation of Natural Frequencies and Buckling Loads for Plane Frames", Int. J. Num. Meth. In Eng., 11, pp. 1067-1081.

55. Howson, W.P., Banerjee, J.R., and Williams, F.W., 1983, "Concise Equations and Program for Exact Eigensolution of Plane Frames Including Member Shear", Adv. Eng. Software, 5(3), pp 137-141.

56. Banerjee, J.R., 2024, "An Exact Method for Free vibration of Beams and Frameworks Using Frequency-Dependent Mass, Elastic and Geometric Stiffness Matrices", Comput. Struct., 292, Paper 107235.

57. Doyle, J.F., 1973, "Approximate Modifications of Stiffness and Carry-Over Factors for Axial Loads and Vibrations", Struct. Engineers, 51(5), pp.183-187.

